Oscillatory Supersonic Kernel Function Method for Interfering Surfaces

Atlee M. Cunningham Jr.*
Convair Aerospace Division of General Dynamics, Fort Worth, Texas

In the method presented in this paper, a collocation technique is used with the nonplanar supersonic kernel function to solve multiple lifting surface problems with interference in steady or oscillatory flow. The pressure functions used are based on conical flow theory solutions and provide faster solution convergence than is possible with conventional functions. In the application of the nonplanar supersonic kernel function, an improper integral of a 3/2 power singularity along the Mach hyperbola is described and treated. The method is compared with other theories and experiment for two wing-tail configurations in steady and oscillatory flow.

Nomenclature

a = freestream speed of sound, m sec
$\bar{a}$ = conical coordinate
AR = aspect ratio
β = supersonic Prandtl-Glauert factor, $\beta^2 = M^2 - 1$
b_{REF} = reference length, meters—usually ½ wing chord for two-dimensional flow or ½ MAC for finite wings in three-dimensional flow
$b(\bar{\eta})$ = wing semichord at span station $\bar{\eta}$, nondimensionalized by b_{REF}
C_p = pressure coefficient, $(p - p_\infty/q)$
$h(\bar{x},\bar{y})$ = mode amplitude at point $\bar{x},\bar{y}$, nondimensionalized by b_{REF}
i = $(-1)^{1/2}$
k = reduced frequency = $(\omega b_{REF}/U)$
m = $(\beta/\tan\Lambda_{LE})$
M = freestream Mach number = (U/a)
MAC = mean aerodynamic chord, meters
$P_q(\bar{\xi},\bar{\eta})$ = supersonic pressure weighting function in the plane of the qth surface, nondimensional
p = pressure, Newtons/meter^2
$\Delta\bar{p}_q(\xi,\eta)$ = lifting pressure amplitude in the plane of the qth surface, Newtons/meter^2
q = freestream dynamic pressure = $(\rho U^2/2)$, Newtons/meter^2
r = $[(y-\eta)^2 + (z-\zeta)^2]^{1/2}$, nondimensionalized by b_{REF}
s_0 = wing semispan, nondimensionalized by b_{REF}
U = freestream velocity, m sec
u,v,w = velocity components in the x,y,z directions, respectively, m sec
$\bar{w}_p(\bar{x},\bar{y})$ = amplitude of the oscillatory downwash normal to the pth surface, m sec
$\bar{W}_p(\bar{x},\bar{y})$ = $8\pi\,\bar{w}_p(\bar{x},\bar{y})/U$
x,y,z = Cartesian coordinate location of the downwash point in the kernel function (x is in the direction of U), nondimensionalized by b_{REF}
$\bar{x},\bar{y},\bar{z}$ = coordinates in the plane of the pth surface with $\bar{z}$ perpendicular (see Fig. 1)
x_0,y_0,z_0 = distance from an influence point to the downwash point, $(x-\xi)$, $(y-\eta)$, $(z-\zeta)$, nondimensional
ΔC_p = lifting pressure coefficient
α = angle of attack, degrees
Λ_{LE}, Λ_{TE} = leading and trailing edge sweep angles, degrees
ξ,η,ζ = location of an influence (or integration) point in the kernel function, nondimensionalized by b_{REF}
$\bar{\xi},\bar{\eta},\bar{\zeta}$ = coordinates in the plane of the qth surface with $\bar{\zeta}$ perpendicular (see Fig. 1)
$\xi_m(\bar{\eta})$ = location of the midchord at span station $\bar{\eta}$, nondimensionalized by b_{REF}
$\bar{\xi},\bar{\eta},\bar{\zeta}$ = $[\bar{\xi} - \xi_m(\eta)/b(\bar{\eta})]$, $\bar{\eta}/s_0$, $\bar{\zeta}/s_0$
$\bar{\eta}_a,\bar{\eta}_b$ = limits of the spanwise integration as determined by geometry and the Mach hyperbola
δ = chordwise variable of integration, nondimensional
ω = rotational frequency, rad/sec

Subscripts

LE = leading edge
MC = Mach cone (or hyperbola) boundary
TE = trailing edge
∞ = freestream conditions
p = downwash surface
q = integration surface

Introduction

REALISTIC prediction of steady or oscillatory aerodynamics on actual airplane configurations requires that equal consideration be given to the interference effects as well as the geometric properties of the lifting surfaces. A pressure function series was introduced in Ref. 1 for isolated trapezoidal wings which was characteristic of supersonic flow by virtue of the weighting function derived from conical flow theory solutions.[2] When used in a collocation technique with the acceleration potential kernel function, the new pressure series converged much faster to the discontinuous solutions characteristic of supersonic flow than a conventional pressure series composed of smooth functions. The rapid convergence was attributed to the fact that the discontinuities were implicit in the new pressure series. Thus, it was felt that the approach of Ref. 1 provided a solid basis for developing a method applicable to general planforms with multiple leading and trailing edge breaks.

As has been shown in subsonic flow, the effect of aerodynamic interference between multiple surfaces cannot be ignored.[3-5] The Woodward vortex panel method[6] has been developed for interfering surfaces in either subsonic or supersonic flow. The method is restricted, however, to steady flow. In unsteady flow, Mach box procedures have been developed for T-tails, V-tails, and top-mounted vertical tails[7] as well as wing-tail configurations.[8] The Mach box methods have the disadvantages of 1) requiring a large number of unknown quantities to obtain a solution, 2) using "diaphragm" regions off of the surfaces where the boundary condition of zero pressure difference must be satisfied, and 3) using rectangular boxes which result in jagged leading and trailing edges for swept planforms. In general, the methods are expensive to use and cumbersome to program. A more complete discussion on these and other existing supersonic methods is given in the Introduction of Ref. 1.

Received June 12, 1974. Sponsored by NASA Langley Research Center, Contract NAS1-11565, and Convair Aerospace Division of General Dynamics Independent Research and Development Program.

Index categories: Aeroelasticity and Hydroelasticity; Structural Dynamic Analysis; Aircraft Aerodynamics (Including Component Aerodynamics).

* Project Structures Engineer. Associate Fellow AIAA.

A more direct approach to solving the supersonic interference problem is to develop a supersonic kernel function method similar to that developed in subsonic flow.[5] The nonplanar supersonic kernel function of Harder and Rodden[9] and the supersonic pressure series of Ref. 1 together provide the ingredients for such a method. Early attempts to develop the method with conventional pressure functions, however, revealed that the supersonic kernel function has a nonintegrable singularity of the 3/2 power along the Mach hyperbola for noncoplanar surfaces.[10] The source of this problem and how it could be solved was discussed in Ref. 10.

Presented in this paper is a supersonic kernel function method for predicting steady and oscillatory airloads on multiple surface configurations with interference. The method uses a collocation technique with the supersonic nonplanar kernel function[9] and the supersonic pressure series.[1] A numerical integration technique is developed for evaluating the improper integral of the 3/2 power singularity discussed above. The method is applied to a coplanar wing-tail configuration in steady flow and a noncoplanar wing-tail in oscillatory flow. Comparison of results with those obtained with existing methods shows excellent agreement.

Definition of the Problem

The fundamental problem to be treated in this paper is the development of a technique to solve the integral equation that relates the normal velocity imposed by boundary conditions with the load distribution on an arbitrary array of planar lifting surfaces in supersonic flow. The equation may be written as

$$\frac{\bar{w}_p(x,y,z)}{U} = \frac{1}{4\pi\rho U^2}\sum_{q=1}^{Q}\int_{S_q}\Delta\bar{p}_q(\xi,\eta,\zeta)K(x-\xi, y-\eta, z-\zeta, k, M)ds \quad (1)$$

for Q total surfaces. The downwash $\bar{w}_p(x,y,z)$ is the velocity normal to the pth lifting surface at control point (x,y,z). The function $\Delta\bar{p}_q(\xi,\eta,\zeta)$ is the normal lift distribution on the qth lifting surface at load (or integration) point (ξ,η,ζ). The kernel function $K(\ )$ is the influence function which is actually the velocity field due to an elemental normal load at point (ξ,η,ζ) on the qth surface. The unknown quantity is $\Delta\bar{p}_q(\xi,\eta,\zeta)$ and $\bar{w}_p(x,y,z)$ is prescribed by the boundary conditions on the lifting surface due to surface slope and motion.

The method used to solve Eq. 1 in this paper is based on a collocation technique. The unknown pressure function is assumed to be composed of a series of polynomials weighted by a function that is characteristic of supersonic pressure distributions as developed in Ref. 1. The nonplanar kernel function as given in the Appendix is derived from the formulation of Harder and Rodden[9] for steady and oscillatory supersonic flow. The integration of the pressure-kernel function product is performed in essentially the same manner as done for subsonic flow[5] with exception of the case $p = q$ in Eq. (1) which has already been treated in Ref. 1. The development of the necessary equations for $p \neq q$ is presented in the following paragraphs.

Assumed Pressure Function

For the qth surface, the pressure function is assumed as a series

$$\Delta\bar{p}_q(\bar{\xi},\bar{\eta}) = qP_q(\tilde{\xi},\tilde{\eta})[g_{0_q}(\bar{\eta})f_0(\bar{\xi}) + g_{1_q}(\bar{\eta})f_1(\bar{\xi}) + \ldots] \quad (2a)$$

where

$$g_{n_q}(\bar{\eta}) = [a_{n0_q}U_0(\bar{\eta}) + a_{n1_q}U_1(\bar{\eta}) + \ldots] \quad (2b)$$

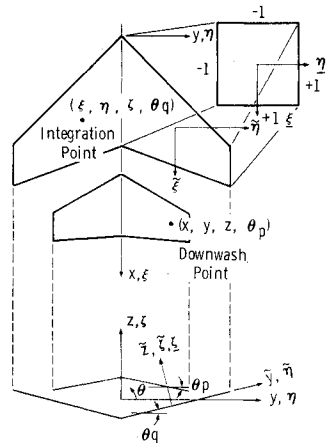

Fig. 1 Basic geometry and coordinate systems for a wing and tail.

$$f_0(\bar{\xi}) = U_0(\bar{\xi}) = 1.0 \quad (2c)$$

$$f_n(\bar{\xi}) = U_n(\bar{\xi}) + U_{n-1}(\bar{\xi}), n > 0 \quad (2d)$$

$U_n(\bar{x})$ = Tschebychev polynomial of the second kind.

The function $P_q(\tilde{\xi},\tilde{\eta})$ is the supersonic weighting function described in Ref. 1. The coordinates, $\tilde{\xi}$, $\tilde{\eta}$, $\bar{\xi}$ are defined in the plane of the qth surface with $\tilde{\zeta}$ perpendicular to the surface as shown in Fig. 1. For mathematical convenience, the pressure function is now defined in the coordinates in the plane of the qth integration surface.

The supersonic weighting function[1] is based on conical flow theory solutions to the lift distributions on flat swept wings.[2] Some liberty was taken to simplify the expressions and yet maintain the basic characteristics. The function has been developed only for simple trapezoidal wings; however, the extension to a general trapezoidal element is currently under development.

Kernel Function

The kernel function, $K(\ )$ shown in Eq. (1) is quite complicated but can be reduced to simple form if $k = 0$ (steady flow). Under such conditions, the nonplanar function is expressed as follows:

$$K(x-\xi, y-\eta, z-\zeta, 0, M) = -\frac{2x_0}{r^2R}\left[T_1 - T_2\left(\frac{2}{r^2} - \frac{\beta^2}{R^2}\right)\right], x_0 \geq \beta r$$
$$= 0, x_0 < \beta r \quad (3)$$

where

$$x_0 = x - \xi$$
$$y_0 = y - \eta$$
$$z_0 = z - \zeta$$
$$r^2 = y_0^2 + z_0^2$$
$$R^2 = x_0^2 - \beta^2 r^2$$
$$\beta^2 = M^2 - 1$$
$$T_1 = \cos(\theta_p - \theta_q)$$
$$T_2 = (z_0\cos\theta_p - y_0\sin\theta_p)(z_0\cos\theta_q - y_0\sin\theta_q)$$

(see Fig. 1 for definitions of θ_p and θ_q). The characteristics of the nonplanar supersonic kernel function are identical to those of the subsonic kernel for large values of x_0. For small values of x_0, particularly for $x_0 \approx \beta r$, the differences are of major importance. Although it is not obvious, the kernel has a 3/2 singularity along the Mach hyperbola if, for example, $z_0 \neq 0$ and $\theta_p = \theta_q = 0$. This characteristic leads to an improper integral in the evaluation of Eq. (1) which requires special treatment in a manner analogous to

Mangler's treatment of the spanwise singularity in subsonic flow.[11] The integration technique developed in the next section will be applicable to both steady and oscillatory flow.

The unsteady form of the kernel function is more complicated than that of steady flow and is given in the Appendix. The singularities are similar to those of steady flow and may be integrated in essentially the same manner as was shown for subsonic flow in Ref. 5. The only exception, like subsonic flow, is a logarithmic singularity in the integrand of the spanwise integral encountered only in unsteady flow.

Self-Induced Downwash

The self-induced downwash produced by a lifting surface in supersonic flow is calculated in the manner described in Ref. 1. The only exception is for a surface which has a nonzero value of θ, then the image surface-induced downwash is calculated in the same manner as for $\theta = 0$ but the nonplanar kernel function is used instead of the planar form.

Interference Effects

The calculation of interference effects in supersonic flow is almost identical to that for subsonic flow.[5] The chordwise integration presented in Ref. 1 is directly applicable with the addition of a term to account for the 3/2 power singularity along the Mach hyperbola. The spanwise integral requires treatment of the nonplanar kernel function such that it converges to the coplanar case as the surfaces become coplanar as shown in Ref. 5 for subsonic flow.

Chordwise Integration

The form of the integral equation for parallel nonplanar surfaces in steady supersonic flow is

$$\bar{w}_p(\tilde{x},\tilde{y}) = -\frac{U}{4\pi\rho}\oint_{\tilde{\eta}_a}^{\tilde{\eta}_b}\oint_{\tilde{\xi}_{LE}}^{\tilde{\xi}_{MC}} \Delta\bar{p}_p(\bar{\xi},\bar{\eta})\frac{2x_0}{r^2R}\times\left[1-\frac{2z_0^2}{r^2}+\frac{z_0^2\beta^2}{R^2}\right]d\tilde{\xi}\,d\tilde{\eta} \quad (4)$$

where $\tilde{\eta}_a$ and $\tilde{\eta}_b$ are the left- and right-hand limits of integration defined by wing geometry and the Mach hyperbola. If the chordwise integration is carried out to the Mach hyperbola, a 3/2 singularity is encountered of the form

$$\lim_{\tilde{\xi}\to\tilde{\xi}_{MC}}\left[(x-\xi)^2-\beta^2r^2\right]^{-3/2}$$

Hence, the finite value of the improper integral must be taken.

In order to determine the finite value of the integral, the differentiation of the potential equation for the downwash must be considered. Let the downwash be expressed as the following simplified form:

$$w(x,y) = \frac{\partial}{\partial z}\int_{\eta_a}^{\eta_b}\int_{\xi_{LE}}^{\xi_{MC}}\Delta p(\xi,\eta)\phi(x,\xi,y,\eta,z,0)\,d\xi\,d\eta \quad (5)$$

where $\phi(\ )$ is the potential at point (x,y,z) due to a point load at $(\xi, \eta, 0)$. Since the differential operator is outside the integral sign, Leibnitz's rule must be used to perform the operation

$$\frac{d}{dt}\int_{a(t)}^{b(t)} g(x,t)\,dx = g[b(t),t]\frac{\partial b(t)}{\partial t} - g[a(t),t]\frac{\partial a(t)}{\partial t} + \int_{a(t)}^{b(t)}\frac{\partial}{\partial t}[g(x,t)]\,dx \quad (6)$$

The limits $a(t)$ and $b(t)$ are constant in subsonic and coplanar supersonic flow; thus, their derivatives are zero. For the supersonic noncoplanar case, however, the derivatives are not zero. Since the chordwise term is of much greater importance for interference effects, only the derivatives resulting from the variation of ξ_{mc} with z will be accounted for.

For the chordwise integral, $G(y,\eta)$, a constant pressure distribution, Δp, will be assumed for simplicity. The integral may then be expressed as

$$G(y,\eta) = \Delta p\frac{\partial}{\partial z}\int_{\xi_{LE}}^{\xi_{MC}}\phi(x,\xi,y,\eta,z,0)\,d\xi \quad (7)$$

which, with the application of Eq. (6), becomes

$$G(y,\eta) = \Delta p\left\{\phi(x,\xi_{MC},y,\eta,z,0)\frac{\partial\xi_{MC}}{\partial z} + \int_{\xi_{LE}}^{\xi_{MC}}\frac{\partial}{\partial z}[\phi(x,\xi,y,\eta,z,0)]\,d\xi\right\} \quad (8)$$

For

$$\phi(x,\xi,y,\eta,z,0) = -\frac{2U}{4\pi\rho}\frac{z_0x_0}{r^2R},\quad x_0 \geq \beta r$$

it can be shown (after some algebraic manipulations given in Ref. 10) that the following is true

$$\phi(x,\xi_{MC},y,\eta,z,0)\frac{\partial\xi_{MC}}{\partial z} = \frac{2U}{4\pi\rho}\frac{z_0^2\beta^2}{r^2}\left[\lim_{\xi\to\xi_{MC}}\frac{1}{R}\right] \quad (9)$$

The differentiation inside the integral in Eq. (8) is the kernel function

$$\frac{\partial}{\partial z}\phi(x,\xi,y,\eta,z,0) = -\frac{2U}{4\pi\rho}\frac{x_0}{r^2R}\left[1-\frac{2z_0^2}{r^2}+\frac{z_0^2\beta^2}{R^2}\right] = \frac{U}{4\pi\rho}K(x,\xi,y,\eta,z,0) \quad (10)$$

Combining Eqs. (8–10) and removing the singularity yields

$$G(y,\eta) = \frac{\Delta pU}{4\pi\rho}\left\{\frac{2z_0^2\beta^2}{r^2}\left[\lim_{\xi\to\xi_{MC}}\frac{1}{R}\right] - \oint_{\xi_{LE}}^{\xi_{MC}}\frac{2x_0z_0^2\beta^2}{r^2R^3}\,d\xi + \int_{\xi_{LE}}^{\xi_{MC}}\left[K(x,\xi,y,\eta,z,0)+\frac{2x_0z_0^2\beta^2}{r^2R^3}\right]d\xi\right\} \quad (11)$$

But

$$\oint_{\xi_{LE}}^{\xi_{MC}}\frac{2x_0z_0^2\beta^2}{r^2R^3}\,d\xi = \frac{2z_0^2\beta^2}{r^2}\left[\lim_{\xi\to\xi_{MC}}\left(\frac{1}{R}\right)-\frac{1}{R_{LE}}\right]$$

Thus, Eq. (11) becomes

$$G(y,\eta) = \frac{\Delta pU}{4\pi\rho}\left\{\frac{2z_0^2\beta^2}{r^2R_{LE}} + \int_{\xi_{LE}}^{\xi_{MC}}\left[K(x,\xi,y,\eta,z,0)+\frac{2x_0z_0^2\beta^2}{r^2R^3}\right]d\xi\right\}$$

which is the final form for the chordwise integral with a constant pressure distribution. For a variable $\Delta p(\xi, \eta)$, the singularity is treated at the Mach hyperbola; hence

$$G(y,\eta) = \frac{U}{4\pi\rho}\left\{\frac{2z_0^2\beta^2}{r^2R_{LE}}\Delta p(\xi_{MC},\eta) + \int_{\xi_{LE}}^{\xi_{MC}}\left[\Delta p(\xi,\eta)K(x,\xi,y,\eta,z,0)+\frac{2x_0z_0^2\beta^2}{r^2R^3}\Delta p(\xi_{MC},\eta)\right]d\xi\right\}$$

Thus, for steady or unsteady interference of nonplanar surfaces the quadrature integration[1] of the chordwise integral becomes

$$G_q(\bar{y},\bar{\eta}) = b(\tilde{\eta})\frac{(1+\bar{\xi}_{MC})}{2}\frac{\pi}{J}\sum_{j=1}^{J}(1-\delta_j^2)^{1/2}\Delta\bar{p}_q(\bar{\xi}_j,\eta)K(x$$

$$- \xi_j, y - \eta, z - \zeta, k, M) + T_2 \Delta\bar{p}_q(\bar{\xi}_{MC}, \bar{\eta}) \frac{2z_0^2\beta^2}{r^2} \left\{ \frac{1}{R_{LE}} + b(\tilde{\eta}) \frac{\pi}{J} \sum_{j=1}^{J} \frac{(1 - \delta_j^2)^{1/2}}{R_j^3} \right\}, \xi_{MC} < 1 \quad (12)$$

where T_2 is defined for Eq. (3) and

$$R_j^2 = (x - \xi_j)^2 - \beta^2 r^2$$

$$\delta_j = -\cos\left(\frac{2j-1}{2J}\pi\right), \quad j = 1, 2, \ldots J$$

$$\bar{\xi}_j = \frac{1}{2}[(1 + \xi_{MC})\delta_j + (\xi_{MC} - 1)]$$

$$\xi_j = [\bar{\xi}_j b(\tilde{\eta}) + \xi_m(\tilde{\eta})]$$

For the case of the Mach hyperbola falling aft of the trailing edge, the 3/2 singularity need not be considered. Hence, the chordwise integral takes on the form given in Ref. 1

$$G_q(\bar{y}, \bar{\eta}) = b(\tilde{\eta}) \frac{\pi}{J} \sum_{j=1}^{J} (1 - \bar{\xi}_j^2)^{1/2} \Delta\bar{p}_q(\bar{\xi}_j, \bar{\eta}) K(x - \xi_i, y - \eta, z - \zeta, k, M), \xi_{MC} \geq 1 \quad (13)$$

where

$$\bar{\xi}_j = -\cos\left(\frac{2j-1}{2J}\pi\right), j = 1, 2, \ldots J$$

In the existing method, no special treatment of pressure function discontinuities in the integrand has been made. The means of evaluating the integral simply depends upon the use of at least twenty or more chordwise integration points, i.e., $J \geq 20$. A scheme is under development, however, which will reduce the nominal value of J by a factor of two to four depending on the value of the reduced frequency, k. For $k \ll 1.0$, the factor would be about four and for $k \sim 1.0$, it would be about two. The reduction in required integration points will result in a substantial savings for oscillatory flow problems due to the reduction in the number of times that the unsteady kernel function must be evaluated.

Spanwise Integration

The spanwise integral for nonplanar interfering surfaces may be written as

$$I_q(\bar{y}) = \oint_{\bar{\eta}_a}^{\bar{\eta}_b} H_q(\bar{y}, \bar{\eta}) \left[\frac{T_1}{r^2} - \frac{2T_2}{r^4} \right] \quad (14)$$

where the sign $\oint$ denotes a "Pseudo Mangler" evaluation of the integral as discussed in Ref. 5. The $H_q(\bar{y}, \bar{\eta})$ function is the modified chordwise integral

$$H_q(\bar{y}, \bar{\eta}) = \frac{G_q(\bar{y}, \bar{\eta})}{\left[\frac{T_1}{r^2} - \frac{2T_2}{r^4} \right]} \quad (15)$$

which will be expanded as

$$H_q(\bar{y}, \bar{\eta}) = H_q(\bar{y}, \bar{y}) + (\bar{\eta} - \bar{y}) H_q'(\bar{y}, \bar{y}) + \ldots$$

Following the developments of Refs. 1 and 5, the spanwise integral is evaluated as

$$I_q(\bar{y}_r) = \frac{\pi}{S} \sum_{s=1}^{S} h(\bar{\eta}_s) H_q(\bar{y}_r, \bar{\eta}_s) + Q_q^S(\bar{y}_r) \quad (16a)$$

where $h(\bar{\eta}_s)$ and $\bar{\eta}_s$ are defined in Ref. 1,

$$Q_q^S(\bar{y}_r) = H_q(\bar{y}_r, \bar{y}_r)[F_1(\bar{y}_r)\cos(\theta_p - \theta_q) + F_3(\bar{y}_r)\sin(\theta_p - \theta_q)] + H_q'(\bar{y}_r, \bar{y}_r)[F_2(\bar{y}_r)\cos(\theta_p - \theta_q)] \quad (16b)$$

and

$$F_1(\bar{y}_r) = \left[\frac{\bar{y}_r - \bar{\eta}_b}{r_{rb}^2} - \frac{\bar{y}_r - \bar{\eta}_a}{r_{ra}^2} \right] - \frac{\pi}{S} \sum_{s=1}^{S} h(\bar{\eta}_s) \left[\frac{1}{r_{rs}^2} - \frac{2\bar{z}^2}{r_{rs}^4} \right] \quad (16c)$$

$$F_2(\bar{y}_r) = \frac{1}{2} \ln \left| \frac{r_{rb}^2}{r_{ra}^2} \right| + \bar{z}^2 \left[\frac{1}{r_{rb}^2} - \frac{1}{r_{ra}^2} \right] - \frac{\pi}{S} \sum_{s=1}^{S} h(\bar{\eta}_s)(\bar{\eta}_s - \bar{y}_r) \left[\frac{1}{r_{rs}^2} - \frac{2\bar{z}^2}{r_{rs}^4} \right] \quad (16d)$$

$$F_3(\bar{y}_r) = \bar{z} \left[\frac{1}{r_{rb}^2} - \frac{1}{r_{ra}^2} \right] - \frac{\pi}{S} \sum_{s=1}^{S} h(\bar{\eta}_s) \frac{\bar{z}(\bar{y}_r - \bar{\eta}_s)}{r_{rs}^4} \quad (16e)$$

The variables $(\bar{y}, \bar{\eta}, \bar{z})$ are all measured relative to the surface over which the integration is being performed as shown in Fig. 1. The perpendicular distance from the surface to the downwash point is $\bar{z}$ and it is measured at span station $\bar{y}$. The terms r_{ra}, r_{rb}, r_{rs} are

$$r_{ra}^2 = (\bar{y}_r - \bar{\eta}_a)^2 + \bar{z}^2 \quad (17a)$$

$$r_{rb}^2 = (\bar{y}_r - \bar{\eta}_b)^2 + \bar{z}^2 \quad (17b)$$

$$r_{rs}^2 = (\bar{y}_r - \bar{\eta}_s)^2 + \bar{z}^2 \quad (17c)$$

This completes the equations necessary to perform the spanwise integration for interference effects due to a streamwise planar surface of arbitrary orientation in steady flow.

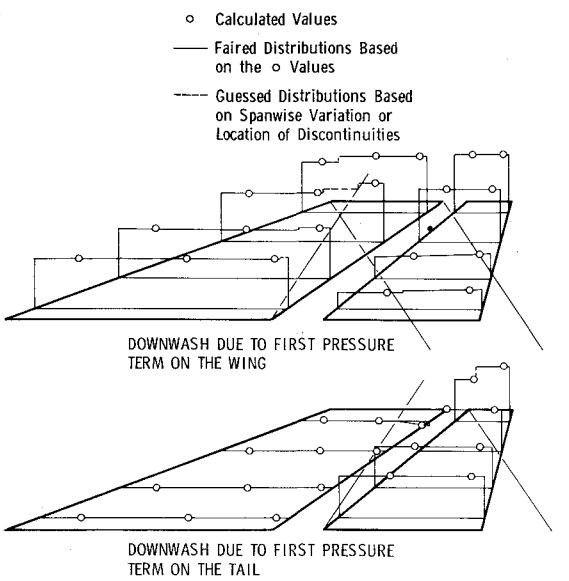

Fig. 2 Induced downwash on an AGARD coplanar wing-tail configuration in steady flow, $M = 1.2$.

Shown in Fig. 2 is an example of calculated downwash distributions on a wing-tail configuration for the first pressure term in both the wing and tail pressure series. These terms correspond to the supersonic weighting function in either case. As can be seen, the downwash distributions are quite flat and well behaved with exception of the jump in the tip Mach cone on the horizontal tail.

For unsteady flow, it is necessary to include additional terms which account for the logarithmic singularity in the spanwise integrand, $k^2 \ln|r|$. This singularity is relatively weak for most problems, i.e., $k < 1$. The correction terms developed in subsonic flow[5] are applicable in this case. The spanwise integration function, $h(\bar{\eta}_s)$, is given in Ref. 1 [Eq. (17)]. The form for the unsteady correction terms becomes

$$Q_q^U(y_r) = Q_q^S(y_r) + \frac{k^2}{2}\cos(\theta_p - \theta_q) \left\{ H_q(\bar{y}_r, \bar{y}_r) \left[J_1(\bar{y}_r) - \frac{\pi}{S} \sum_{s=1}^{S} h(\bar{\eta}_s) \ln r_{rs}^2 \right] + H_q'(\bar{y}_r, \bar{y}_r) \left[J_2(\bar{y}_r) - \frac{\pi}{S} \sum_{s=1}^{S} h(\bar{\eta}_s)(\bar{\eta}_s - \bar{y}_r) \ln r_{rs}^2 \right] \right\} \quad (18a)$$

where

$$J_1(\bar{y}_r) = (\bar{y}_r - \bar{\eta}_a)\ln r_{ra}^2 - (\bar{y}_r - \bar{\eta}_b)\ln r_{rb}^2 + 2|\bar{z}_0|\left[\tan^{-1}\left(\frac{\bar{y}_r - \bar{\eta}_a}{|\bar{z}_0|}\right) + \tan^{-1}\left(\frac{\bar{\eta}_b - \bar{y}_r}{|\bar{z}_0|}\right)\right] - 4 \quad (18b)$$

$$J_2(\bar{y}_r) = -\frac{1}{2}[r_{ra}^2 \ln r_{ra}^2 - r_{rb}^2 \ln r_{rb}^2] + \bar{\eta}_a + \bar{\eta}_b - 2\bar{y}_r \quad (18c)$$

which completes the equations for unsteady flow.

Solving the Boundary Value Problem

The boundary value problem is solved in the usual manner for either steady or unsteady flow by equating the calculated downwash from the pressure assumed functions to that prescribed by the boundary conditions. The vector of unknown pressure series coefficients, $\{a_{nmq}\}$, in Eq. (2b) are solved for as follows:

$$\{a_{nmq}\} = -q\pi[A]^{-1}\left\{\frac{\partial h(\tilde{x}_i, \tilde{y}_r)}{\partial \tilde{x}}_p + ikh(\tilde{x}_i, \tilde{y}_r)_p\right\}$$

where $[A]$ is the matrix of influence coefficients as derived from the evaluation of Eq. (1). The locations of the control points on each surface are prescribed as

$$\bar{x}_i = -\cos\left(\frac{2i\pi}{2NC_p + 1}\right), \quad i = 1, 2, \ldots NC_p$$

$$\bar{y}_r = \cos\left(\frac{r\pi}{2NS_p + 1}\right), \text{ Rectangular}$$

$$\bar{y}_r = \cos\left(\frac{r\pi}{NS_p + 1}\right), \text{ Swept} \quad r = 1, 2, \ldots (NS_p = R)$$

where the transformation from $\bar{x}_i$ to $\tilde{x}_i$ is the same as that for $\bar{\xi}_j$ to $\tilde{\xi}_j$ is given for Eq. (12). The $\tilde{x}_i$ and $\tilde{y}_r$ are coordinates in the system coplanar with the pth surface. NC_p and NS_p are the number of chordwise and spanwise functions used to describe the pressure distributions. For more discussion on relationships between (NC_p, NS_p) and (NC_q, NS_q), the reader is referred to Ref. 5.

Numerical Results

Two examples of application of the supersonic method are shown in Figs. 3 and 4. These results are preliminary in nature and are presented to verify that two objectives have been achieved. The first is that the use of the nonplanar supersonic kernel function in a collocation technique is shown to be a valid means for treating problems with interfering surfaces. The second is that the validity is established for the chordwise integration technique that accounts for the 3/2-power singularity along the Mach hyperbola.

The first example in Fig. 3 is a case in which the AGARD wing-tail configuration is at $\alpha = 1.0$ radian in steady $M = 1.20$ flow. The number of terms used are $NS = 4$ (spanwise) on both the wing and tail and $NC = 3$ (chordwise) on the wing and $NC = 2$ on the tail. The results shown as solid curves are compared with results from the Woodward method[6] as indicated by the symbols. The disagreement at the wing and tail tips is due to the inability of the Woodward method to predict these discontinuities with a reasonable number of vortex panels.

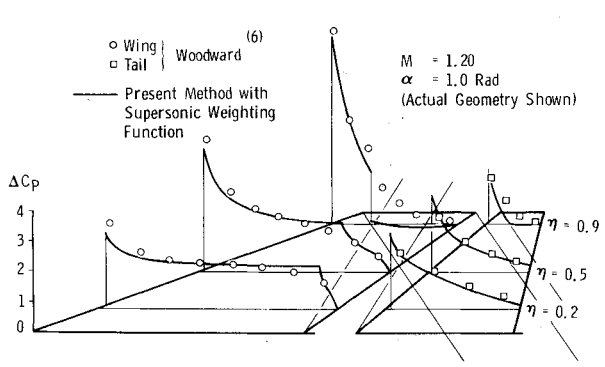

Fig. 3 Steady lift distribution on the AGARD coplanar wing-tail configuration.

The second example in Fig. 4 is a case for a noncoplanar rectangular wing and tail. The wing is oscillating in a uniform translation mode at $k = 0.2$ (based on semispan) and $M = 1.20$ flow. The tail is stationary. The results of the present method (solid and dashed curves) are compared with those obtained by the AFFDL Mach Box method[8] (symbols). Both real and imaginary parts of the solution are shown. The number of terms used were NC = 3 and NS = 4 on both the wing and tail for a total cost of about 3½ min on an IBM 370/155. The Mach Box solution used 189 boxes on the wing, tail, and in the diaphragms. This particular case led to the discovery of the chordwise integration problem since the Mach hyperbola for leading edge control points on the tail fell forward of the wing trailing edge. Not accounting for the improper integral produced singular pressures on the tail which were opposite in sign to Mach Box pressures along the tail leading edge. Hence, the investigation of this phenomenon was pursued as discussed in Ref. 10. As shown by the final results in Fig. 4, the chordwise integration technique is a valid treatment of the 3/2 singularity along the Mach hyperbola.

Conclusions

In this paper a supersonic kernel function method has been presented for predicting steady and oscillatory airloads on multiple surface configurations with interference. The method uses a collocation technique with assumed pressure functions and the supersonic nonplanar kernel function. The pressure functions which were developed originally for isolated wings[1] are weighted by approximations to conical flow theory solutions for the flat plate trapezoidal wing problem, hence, the first term in the pressure series is nearly an exact solution for uniform angle of attack. A numerical integration technique has been developed for evaluating the improper integral of the 3/2 power singularity in the kernel function that exists along the Mach hyperbola for noncoplanar configurations.

The method was used to obtain preliminary results for wing-tail configurations in steady and unsteady flow which are also coplanar and noncoplanar. These results were very encouraging and will provide momentum for refining the method into an efficient practical computer program. The principal refinements will be involved with improving the integration schemes such that coarser inte-

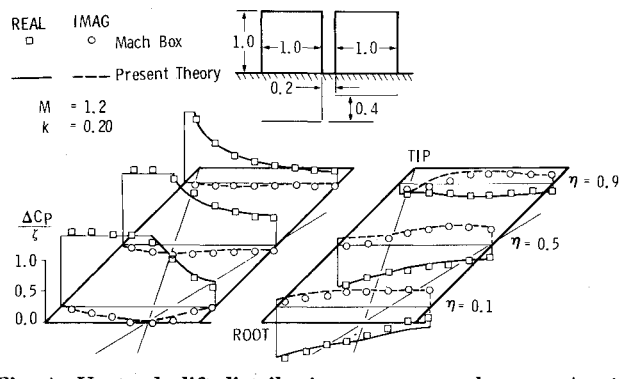

Fig. 4 Unsteady lift distribution on a noncoplanar rectangular wing and tail configuration due to a unit wing translation mode.

gration grids may be used and modification of the pressure functions such that configurations with intersecting surfaces (T-Tails and Wing-Pylon combinations) can be more easily treated.

Appendix

The nonplanar kernel function for unsteady supersonic flow has been given by Harder and Rodden[9] in the following form

$$K(x-\xi, y-\eta, z-\zeta, k, M) = -\frac{e^{-ikx_0}}{r^2}\left[K_1T_1 + \frac{K_2T_2}{r^2}\right], \quad -x_0 \geq \beta r$$
$$= 0, \quad x_0 < \beta r \qquad \text{(A1)}$$

where all of the terms have been previously defined [for Eq. (3)] with the exception of the K_1 and K_2 terms.

The K_1 and K_2 terms as defined by Harder and Rodden have been modified to a more convenient form similar to that presented in Ref. 5 in subsonic flow. The K_1 term is expressed as

$$K_1 = K_{11} + K_{12} \qquad \text{(A2a)}$$

where

$$K_{11} = \left(\frac{x_0}{R} + 1\right)e^{-ikru_1} - I_{11} \qquad \text{(A2b)}$$

$$K_{12} = \left(\frac{x_0}{R} - 1\right)e^{-ikru_2} + I_{12} \qquad \text{(A2c)}$$

$$u_1 = \frac{x_0 - MR}{\beta^2 r} \qquad \text{(A3a)}$$

$$u_2 = \frac{x_0 + MR}{\beta^2 r} \qquad \text{(A3b)}$$

$$\beta^2 = M^2 - 1$$

For $u_1 \geq 0$,

$$I_{11} = ikre^{-ikru_1}\sum_{n=1}^{11}\frac{a_nE_1{}^n}{nc + ikr} \qquad \text{(A4a)}$$

or for $u_1 < 0$,

$$I_{11} = ikre^{-ikru_1}\sum_{n=1}^{11}\frac{a_nE_1{}^n}{nc - ikr} + 2\left[e^{-ikru_1} - 1 + (kr)^2\sum_{n=1}^{11}\frac{a_n}{(nc)^2 + (kr)^2}\right] \qquad \text{(A4b)}$$

and

$$I_{12} = ikre^{-ikru_2}\sum_{n=1}^{11}\frac{a_nE_2{}^n}{nc + ikr} \qquad \text{(A4c)}$$

where

$$E_1 = e^{-c|u_1|} \qquad \text{(A4d)}$$

$$E_2 = e^{-cu_2} \qquad \text{(A4e)}$$

$$c = 0.372$$

For the K_2 term, the following expressions are used in Eq. (A1):

$$K_2 = K_{21} + K_{22} \qquad \text{(A5a)}$$

where

$$K_{21} = 3I_{11} - I_{21} - \left\{2\left(\frac{x_0}{R} + 1\right) + \frac{r^2}{R^2}\left[\frac{\beta^2 x_0}{R} + \frac{ikrM^2}{(1 + u_1{}^2)^{1/2}}\right]\right\}e^{-ikru_1} \qquad \text{(A5b)}$$

$$K_{22} = -3I_{12} + I_{22} - \left\{2\left(\frac{x_0}{R} - 1\right) + \frac{r^2}{R^2}\left[\frac{\beta^2 x_0}{R} - \frac{ikrM^2}{(1 + u_2{}^2)^{1/2}}\right]\right\}e^{-ikru_2} \qquad \text{(A5c)}$$

For $u_1 \geq 0$,

$$I_{21} = ikre^{-ikru_1}\sum_{n=1}^{11}\frac{b_nE_1{}^{2n}}{2nc + ikr} \qquad \text{(A6a)}$$

or for $u_1 < 0$,

$$I_{21} = ikre^{-ikru_1}\sum_{n=1}^{11}\frac{b_nE_1{}^{2n}}{2nc - ikr} + 2\left[e^{-ikru_1} - 1 + (kr)^2\sum_{n=1}^{11}\frac{b_n}{(2nc)^2 + (kr)^2}\right] \qquad \text{(A6b)}$$

and

$$I_{22} = ikre^{-ikru_2}\sum_{n=1}^{11}\frac{b_nE_2{}^{2n}}{2nc + ikr} \qquad \text{(A6c)}$$

The a_n and b_n coefficients in the series summations in Eqs. (A4) and (A6) are given in Table 1. The a_n set are those given originally by Laschka[3] for the approximation

$$\frac{u}{(1 + u^2)^{1/2}} - 1 \approx \sum_{n=1}^{11} a_ne^{-ncu} \qquad \text{(A7a)}$$

The b_n set are those given by Cunningham[5] for the approximation

$$\frac{u^3}{(1 + u^2)^{3/2}} - 1 \approx \sum_{n=1}^{11} b_ne^{-2ncu} \qquad \text{(A7b)}$$

Table 1 Kernel function series coefficients

n	a_n	b_n
1	−0.24186198	−3.509407
2	2.7968027	57.17120
3	−24.991079	−624.7548
4	111.59196	3830.151
5	−271.43549	−14538.51
6	305.75288	35718.32
7	41.183630	−57824.14
8	−545.98537	61303.92
9	644.78155	−40969.58
10	−328.72755	15660.04
11	64.279511	−2610.093

References

[1]Cunningham, A. M., Jr., "Oscillatory Supersonic Kernel Function Method for Isolated Wings," *Journal of Aircraft*, Vol. 11, No. 10, Oct. 1974, pp. 609–615.

[2]Cohen, D., "Formulas for the Supersonic Loading, Lift and Drag of Flat Swept-Back Wings with Leading Edges Behind the Mach Lines," Rept. 1050, 1951, NACA.

[3]Laschka, B. and Schmid, H., "Unsteady Aerodynamic Forces on Coplanar Lifting Surfaces in Subsonic Flow (Wing-Horizontal Tail Interference)," *Jahrbuch 1967 der WGLR*, pp. 211–222.

[4]Albano, E., Perkinson, F., and Rodden, W. P., "Subsonic Lifting-Surface Theory Aerodynamic and Flutter Analysis of Interfering Wing/Horizontal-Tail Configurations," AFFDL-TR-70-59, Sept. 1970, Air Force Flight Dynamics Lab., Wright-Patterson Air Force Base, Ohio.

[5]Cunningham, A. M. Jr., "A Collocation Method for Predicting Oscillatory Subsonic Pressure Distributions on Interfering Parallel Lifting Surfaces," AIAA Paper 71-329, Anaheim, Calif., 1971.

[6]Woodward, F. A. and Hague, D. S., "A Computer Program for the Aerodynamic Analysis and Design of Wing-Body-Tail Combinations at Subsonic and Supersonic Speeds, Volume I: Theory and Program Utilization," ERR-FW-867, Feb. 1969, Convair Aerospace Div. of General Dynamics, Fort Worth, Texas.

[7]Andrew, L. V., "Unsteady Aerodynamics for Advanced Configurations, Part VI—A Supersonic Mach Box Method Applied to T-Tails, V-Tails, and Top-Mounted Vertical Tails," AFFDL-TDR-64-152, May 1969, Air Force Flight Dynamics Lab., Wright-Patterson Air Force Base, Ohio.

[8]Ii, J. M., Borland, C. J., and Hogley, J. R., "Prediction of Unsteady Aerodynamic Loadings of Non-Planar Wings and Wing-Tail Configurations in Supersonic Flow, Part 1—Theoretical Development, Program Usage and Application," AFFDL-TDR-71-

108, March 1972, Air Force Flight Dynamics Lab., Wright-Patterson Air Force Base, Ohio.

[9]Harder, R. L. and Rodden, W. P., "Kernel Function for Nonplanar Oscillating Surfaces in Supersonic Flow," *Journal of Aircraft*, Vol. 8, No. 8, Aug. 1971, pp. 677–679.

[10]Cunningham, A. M., Jr., "The Application of General Aerodynamic Lifting Surface Elements to Problems in Unsteady Transonic Flow," CR-112264, Feb. 1973, NASA.

[11]Multhopp, H., "Methods for Calculating the Lift Distribution of Wings," (Appendix I, Contributed by W. Mangler), Rept. Aero-2353, January 1950, Royal Aircraft Establishment, Farnborough, Great Britain.

NOVEMBER 1974 J. AIRCRAFT VOL. 11, NO. 11

F-12 Series Aircraft Propulsion System Performance and Development

David H. Campbell*
Lockheed California Company, Burbank, Calif.

The F-12 aircraft propulsion system elements are described. Flight performance of the inlet, engine, and ejector are treated, and the importance of flowfield simulation and engine nacelle leakage are demonstrated. The inlet design philosophy is discussed along with the importance of inlet control to the whole propulsion system. The inlet unstart is described, followed by a brief development history of the control schedules and their effect on the frequency of unstarts. Close cooperation between the airframe and engine manufacturers allowed an interface beneficial to the propulsion system.

Nomenclature

AB = afterburning
G = normal acceleration
Btu = British thermal units
$LVDT$ = linear voltage differential transducer
C_L = lift coefficient based on wing reference area
C_D = drag coefficient based on wing reference area
C_{fp} = ejector gross thrust minus pressure drag over ideal primary gross thrust
rpm = revolutions per minute
α = angle of attack measured from the wing reference plane
Engine Face Mass Flow Ratio = ratio of engine face station mass flow to the flow through an area equal to the inlet capture area at freestream conditions
Engine Face Total Pressure Recovery: total pressure at the engine face station divided by freestream total pressure calculated with a specific heat ratio of 1.4
Distortion: maximum pressure minus minimum pressure divided by the average pressure at the engine face
Mach number: velocity divided by the local speed of sound

Introduction

THE F-12 series of aircraft were designed in the early 1960's by the Advanced Development Projects group (the "Skunk Works") of Lockheed. The YF-12 set speed and sustained altitude records in 1964 which stand unchallenged to this day. These aircraft have unique propulsion system components required for sustained cruise above Mach 3.0 and at altitudes in excess of 80,000 ft. The propulsion system consists of an axisymmetric mixed compression inlet, the Pratt & Whitney J-58 bleed bypass turbojet engine, and a fuselage mounted blow-in-door ejector.

The purpose of this paper is to describe the F-12 propulsion system with particular emphasis upon the airframe mounted components. The airframe portion of this system interacts with the aircraft flowfields to significantly affect the performance of the aircraft in flight. Flight test results have been compared with various ground tests to confirm these effects and will be presented. The aircraft design objectives included efficient high-altitude cruise at maximum or part afterburning power. The aircraft angle of attack range was to be modest so the inlets were expected to accept air over a limited range of angle of attack. At supersonic speeds above Mach 1.6, the inlets operate in the internal compression mode, and supersonic flow within the inlet can become unstable, breaking down in what is known as an inlet unstart. This phenomenon requires careful control of the inlet geometry and the airflow passing through the inlet. The success of this propulsion system in avoiding unstarts is discussed in terms of inlet control; however, the care taken in minimizing engine airflow transients by the engine designers is equally important.

Presented as Paper 73-821 at the AIAA 5th Aircraft Design, Flight Test and Operations Meeting, St. Louis, Mo., August 6–8, 1973; submitted August 20, 1973; revision received July 25, 1974.

Index categories: Airbreathing Propulsion, Subsonic and Supersonic; Aircraft Performance; Aircraft Powerplant Design and Installation.

*Department Manager, Thermo/Propulsion. Associate Fellow AIAA.

Propulsion System Description

The F-12 aircraft (Fig. 1) is clearly dominated by the propulsion system, with nacelles larger in diameter than the basic fuselage. The propulsion system depicted in Fig. 2 is made up of three major elements: 1) inlet and inlet control, 2) engine and its control, and 3) self-actuating airframe mounted ejector nozzle. Ready engine access is provided by hinging the outer wing about the upper outboard nacelle split line. The hinged portion of the nacelle and ejector is depicted separately for clarity.

Inlet

The inlet is axisymmetric with a translating spike. When the spike is retracted to its high Mach number position, the inlet contains an internal throat typical of a mixed compression inlet. Boundary-layer control on the spike is provided by a porous centerbody bleed with the bleed air passing overboard through louvers located at the ends of the centerbody support struts (Fig. 3). Cowl boundary-layer bleed is taken off through a "shock trap" bleed, oversized to provide sufficient pressure to feed the air through the engine secondary compartment and into